RESEARCH ARTICLE

JOURNAL OF Applied Polymer SCIENCE WILEY

Synthesis of an injectable heparin conjugated poloxamer hydrogel with high elastic recoverability for temporomandibular joint disorders

Buse Deliogullari[1] ⓘ | Esra Ilhan-Ayisigi[2,3] ⓘ | Betul Cakmak[2] ⓘ |
Pelin Saglam-Metiner[2] ⓘ | Nusret Kaya[4] ⓘ | Gulcan Coskun-Akar[5] ⓘ |
Ozlem Yesil-Celiktas[1,2] ⓘ

[1]Biomedical Technologies Graduate Programme, Graduate School of Natural and Applied Sciences, Ege University, Bornova, Izmir, Turkey

[2]Department of Bioengineering, Faculty of Engineering, Ege University, Izmir, Turkey

[3]Genetic and Bioengineering Department, Faculty of Engineering and Architecture, Kirsehir Ahi Evran University, Kirsehir, Turkey

[4]Department of Materials Science and Engineering, Faculty of Engineering and Architecture, Izmir Katip Celebi University, Cigli, Izmir, Turkey

[5]Department of Prosthodontics, Faculty of Dentistry, Ege University, Izmir, Turkey

Correspondence
Ozlem Yesil-Celiktas, Biomedical Technologies Graduate Programme, Graduate School of Natural and Applied Sciences, Ege University, Bornova, Izmir, Turkey.
Email: ozlem.yesil.celiktas@ege.edu.tr

Abstract

The temporomandibular joint (TMJ) is commonly affected during fundamental oral activities, reducing the quality of life. Herein, we synthesized a heparin-conjugated poloxamer hydrogel (HEP) as a thermo-responsive injectable hydrogel for the treatment of TMJ disorders. While the gelation temperature of synthesized HEP (25% [w/v]) was 29.8–30.0°C, there was a slight difference between loss and storage modulus. HEP decreased the friction of the TMJ, thus requires less energy during load-bearing jaw movement in comparison to POL. Moreover, the oscillation test dependent on strain ranges from 0.01% to 1000% validated that POL and HEP3 hydrogels showed a similar critical strain of about 5.6%. The total elastic recovery percentage of HEP3 (53.50%) was higher than POL (45.55%), indicating a better recovery of the deformed hydrogel structure. Along with the suitable viscoelastic properties for temporomandibular cavity, both hydrogels increased the proliferation of fibroblasts (L929) and chondrocytes (ATDC5) (cell viabilities were above 100%). However, newly synthesized HEP induced differentiated cell proliferation of chondrogenic cells at increasing concentrations up to 0.0156 mg/mL ($p < 0.0001$) compared to POL and the control group. The promising rheological properties and effects on chondrogenic cell proliferation of injectable heparin-conjugated hydrogel make them candidates for intra-articular injections used for the treatment of TMJ.

KEYWORDS

heparin, injectable hydrogel, poloxamer, temporomandibular joint, temperature sensitive gelation, viscoelastic characterization

1 | INTRODUCTION

Temporomandibular joint (TMJ) disc is a special porous fibrocartilage that has high water content, low friction, and high mechanical strength between the temporal bone and mandible.[1,2] The viscoelastic structure of TMJ disc allows absorption and distribution of stress[3] and provides the crucial point of jaw movement during chewing and speaking.[4] TMJ disorders occur in relation to various psychological, mental, genetic or hormonal reasons such as clenching and grinding, tooth loss, stress and closing disorder. The most common symptom of TMJ disorders is

acute or chronic pain. Although these pain-related disorders are not life threatening, quality of human life, daily activities and psycho-social conditions are adversely affected.[5] The treatment of TMJ disc can vary as non-invasive, minimally invasive and invasive procedures according to the severity of the disorder. Osteoarthritis-like joint disorders of the TMJ disc cause bone and cartilage destruction along with tissue inflammation.[6] When bone and cartilage destruction occurs, the use of autogenous and alloplastic materials to restore the area causes pain in the facial area for a long time, while injections of materials such as anti-inflammatory drugs, Botox, and hyaluronic acid may not be sufficient for treatment. Hence, a longer-lasting treatment can be achieved by injection of a load-bearing yet biocompatible material without surgery.[7] In recent years, injectable hydrogels based on synthetic polymers such as Poloxamer have become frequently preferred for tissue engineering applications due to their high tissue-like water content, easily manipulated physical properties, and minimally invasive delivery.[8–10] Poloxamer hydrogel has a highly lipophilic property that mimics natural extracellular matrix (ECM), not only enhancing cell growth and interaction, but also supporting cell viability.[11] Moreover, Poloxamer 407 is recognized as an "inactive ingredient" by the US Food and Drug Administration for various drugs such as oral solutions, suspensions, inhalation, intravenous, ophthalmic, or topical formulations.[12] By chemical modification of Poloxamer and crosslinking with different molecules,[13] hydrogels with various functionalities can be formulated with higher biocompatibility and durability. Additionally, poloxamer macromers can be synthesized by reaction of poloxamer 407 with acryloyl chloride, and poloxamer hydrogels with tunable water content, melting temperature and crystallinity properties can be prepared by photopolymerization of these macromers.[14] For cartilage tissue engineering applications, studies on heparin-bonded polymers are also promising.[15] Heparin, which is a biocompatible, biodegradable and water-soluble natural glycosaminoglycan, effectively improves wound healing and vascularization, reduces inflammation and acts as a strong anticoagulant that can improve local blood circulation.[16,17] Heparin-based hydrogels synthesized from thiolated heparin and poly(ethylene glycol) diacrylate were reported to be effective for cultivation of hepatocytes and chondrocytes, also ensure cell adhesion and proliferation of human mesenchymal stem cells.[18] In this study, heparin-conjugated Poloxamer has been developed as a thermoresponsive injectable hydrogel with an improved mechanical strength suitable for load-bearing applications, along with biocompatible properties. Moreover, it has also been hypothesized that the developed hydrogel could be an alternative to TMJ disc replacement

materials including temporal myofascial flaps and acellular matrix tissue patches for the treatment of TMJ disorders without any surgical risk or postoperative absorption. Up to date, even though various injectable and self-healable hydrogels have been developed for traumatic spinal cord injury,[19] chondral defect repair,[20] and other cartilage engineering applications,[21] to the best of our knowledge, the rheological properties of these hydrogels were not investigated based on the suitability of injection to TMJ. The chemical structure of synthesized hydrogels was characterized by Fourier transform infrared (FTIR), while their porosity properties were investigated by micro-computed tomography (μ-CT). By performing rheological tests, gelling temperature and viscoelastic properties were determined. Furthermore, in vitro biocompatibility of the synthesized heparin-conjugated Poloxamer hydrogel as an artificial injectable biomaterial was carried out with the MTT and Live&Dead assays.

2 | EXPERIMENTAL SECTION

2.1 | Materials

Poloxamer 407 (P407), 4-(Dimethylamino) pyridine (DMAP, Alfa Aesar), Succinic anhydride (MERCK), Triethylamine (TEA, Carlo Erba), Heparin sodium salt from porcine (H5515-250KU, Sigma-Aldrich), 1-Etil-3-(3-dimethylaminopropyl) carbodiimide hydrochloride (EDC, Sigma-Aldrich), N-Hydroxysulfosuccininimide sodium salt (NHS, Sigma-Aldrich) were used as received. Dulbecco's Modified Eagle Medium: Ham's F12 (DMEM-F12) (D6421) and 3-(4,5-dimethylthiazol-2-yl)-2,5-diphenyl tetrazolium bromide (MTT) (M5655-5X1G) were purchased from Sigma–Aldrich. PBS (phosphate buffer saline) (L1825) was purchased from Merck, Live & Dead kit (L3224) from Invitrogen.

2.2 | Synthesis of injectable heparin conjugated poloxamer hydrogels

Heparin conjugated poloxamer (HEP) hydrogels were synthesized in two stages: carboxylation of poloxamer and subsequent heparin bonding to carboxylated poloxamer by EDC-NHS chemistry. Carboxylation reaction of poloxamer was performed as follows: succinic anhydride and poloxamer were mixed in 1,4-dioxane overnight, subsequently DMAP and TEA were added. After the evaporation of 1,4-dioxane, the remaining pellet was dissolved in chloroform and precipitated with cold ether at a 1:6 volume ratio of chloroform to ether.[22,23] Precipitate was centrifuged (4°C,

3000 g) and left in the desiccator for 3 days to attain carboxylated poloxamer. EDC-NHS reaction was modified from Bobbala and coworkers,[24] where redispersed carboxylated poloxamer in PBS was reacted with 0.75 mmol EDC and 0.25 mmol NHS, along with heparin at specified amounts and mixed using a magnetic stirrer overnight. Heparin:carboxylated poloxamer mass ratios of 0.033:1, 0.066:1 and 0.099:1 were added to the reaction media and the formulations were referred as HEP1, HEP2, and HEP3, respectively. Subsequent to the reaction, HEPs were dialyzed in distilled water to remove any unreacted residues for 3 days, and lyophilized (Figure S1).

2.3 | Characterization of hydrogels

2.3.1 | Fourier transform infrared spectrometry

The functional groups of POL, untreated heparin and heparin conjugated poloxamers (HEP) were analyzed by Fourier transform infrared spectroscopy at Ege University Central Research Test and Analysis Laboratory (Ege-MATAL). FTIR spectra of lyophilized samples were recorded between 4000 and 400 cm^{-1} using Perkin-Elmer Spectrum Two instrument.

2.3.2 | Determination of heparin amount by toluidine blue assay

Toluidine Blue Assay was used to determine the amount of heparin bond to poloxamer.[25] Briefly, 0.05 g Toluidine Blue was dissolved in 1 L 0.01 M HCl containing 0.2% NaCl. Different concentrations of 1 ml of untreated standard heparin or sample of HEP were placed in tubes and mixed with 3 ml of Toluidine Blue solution. The tubes were vortexed for 30 s and left in the water bath for 3 h at 37°C. Then, 2 ml of hexane was added to each tube and agitated for 30 s to separate the heparin-dye complex. After 20 min of sedimentation, the colored liquid part was diluted in half with 0.9% NaCl and absorbance was measured by UV-spectrometer at 629 nm.

2.3.3 | Micro-computed tomography analysis

The porosity and pore volume of the samples were analyzed with micro-computed tomography (μ-CT) using Scanco μCT-50 (Scanco Medical AG) at 30°C. The POL and HEP3 hydrogels were scanned with a voxel resolution and 3D images of the hydrogel structure were created from 2D images. Because μ-CT also allows

quantitative analysis of three-dimensional morphology, the experiments were carried out in triplicates of each hydrogels for the representation of data as the mean ± SD. Then, data were analyzed statistically with ANOVA, Tukey's Multiple Comparison Test with a confidence interval of ±95% (p < 0.05) by GraphPad Prism 8.3.0.

2.3.4 | Determination of rheological properties

Viscosity analyses of POL and HEP3 were performed at temperatures from 20°C to 37°C using a viscometer (Brookfield Ametek) in the incubator (37°C) at a speed of 50 rpm for different concentrations (20%, 25%, and 30% w/v). During the monitoring of the viscosity, the temperature difference of the solution was also followed by a digital thermometer, as the sudden increase of viscosity pointed to the gelation temperature of the related solution. The gelation temperatures of hydrogels were also confirmed using the magnetic stirrer method.[26] Briefly, POL and HEP3 solutions at the same concentrations (20%, 25%, 30% w/v) were placed into the glass transparent vials with a digital thermometer, then started stirring on the magnetic stirrer. When the magnetic bar stopped stirring, the observed temperature of the solution was recorded as the gelation temperature.

The viscoelastic properties of hydrogels were studied at a temperature of 37°C in a rheometer (Discovery HR-2, Hybrid rheometer) with a parallel plate configuration at a diameter of 20 mm and a gap size of 1 mm. All experiments were conducted by releasing 1000 μl 25% (w/v) POL and HEP3 hydrogels separately on top of the rheometer plate using a syringe.

2.3.5 | Biocompatibility of hydrogels

The cytotoxicities of 25% (w/v) POL and HEP3 hydrogels on healthy mouse connective subcutaneous tissue fibroblasts (L929) and a differentiated chondrogenic cell line from mouse teratocarcinoma cells (ATDC5) (ATCC) were determined by the MTT assay quantitatively and Live&Dead assay qualitatively on day 3. Before cell seeding, L929 and ATDC5 were maintained in DMEMF12 medium containing 10% (v/v) Fetal Bovine Serum (FBS), 1% (v/v) L-glutamine (200 mM), 0.1% (v/v) gentamicin (10 mg/mL) and 0.1% (v/v) penicillin/streptomycin (10.000 U) in 75-cm^2 cell culture flasks at humidified incubator (5% CO$_2$, 37°C). The MTT assay is a colorimetric experiment that measures the activity of

mitochondrial cells as an index of their viability and proliferation. This test detects only living cells, and the signal produced is directly proportional to the number of living cells.[27] For this, L929 and ATDC5 cells were seeded in 96-well plates (1×10^4 cells/well) as triplicates and incubated at 37°C, 5% CO_2 for 24 h. Then, the cell medium was removed and different concentrations (0.0313; 0.0156; 0.0078; 0.0039 mg/mL) of filter sterilized POL and HEP3 hydrogels (25% w/v) in growth media were added as 100 µl to each well. The reason for using different concentrations of POL and HEP3 hydrogels was to account for the different extent of disk deformation at different stages of TMJ disease. DMEM-F12 medium containing hyaluronic acid at a concentration of 1 mg/ml representing the minimum amount in a patient with temporomandibular joint disc injury, was added to the wells.[28] Cells treated with growth medium and dimethyl sulfoxide (DMSO) were considered as positive and negative controls, respectively. After 72 h of incubation, supernatants were removed and 100 µl of 10% MTT solution (diluted in growth medium from 5 mg/ml stock solution,) was added to each well. Then the plate was incubated at 37°C for 3 h, the MTT solution was removed and 100 µl of DMSO was added to each well. After shaking, the absorbance at 570 nm was measured with a microplate reader (BioTek). Cell viability (%) was calculated with the GraphPad Prism 8.3.0 program.

For Live/Dead analysis, calcein AM/ethidium homodimer-1 was used to investigate the effect of POL and HEP3 hydrogels on viability of cells. Calcein AM, which hold on to living cells, produces green fluorescence, while EthD-1 binds to nucleic acids in damaged cells, showing dead cells in red fluorescent color.[29] ATDC5 and L929 cells were seeded in 48-well plates (2×10^4 cells/well) as triplicate and incubated for 24 h at 37°C, 5% CO_2. Then the cell medium was removed and different concentrations (0.0313; 0.0156; 0.0078; 0.0039 mg/ml) of filter sterilized POL and HEP3 hydrogels (25% w/v) in growth media were placed in each well. After 72 h of incubation, cells were washed with PBS (1X), stained with 2 µM Calcein AM, and 4 µM EthD-1 solution prepared in PBS (1X) and incubated at room temperature (RT) for 60 min in dark. Then cells were washed with PBS (1X) and visualized by fluorescence microscopy (Zeiss, Axio Vert.A1).

2.4 | Statistical analysis

Cell viabilities data were analyzed statistically with One-way ANOVA, Tukey's Multiple Comparison Test with a confidence interval of ±95% ($p < 0.05$) by GraphPad Prism 8.3.0. In order to indicate different levels (degree) of significance, ns; $p > 0.05$, *$p < 0.05$, **$p < 0.01$, ***$p < 0.001$, ****$p < 0.0001$ were used. Data were presented as the mean ± SD (n = 3).

3 | RESULTS AND DISCUSSION

3.1 | Synthesis and characterization of injectable heparin conjugated poloxamer hydrogels

The heparin conjugated poloxamer (HEP) was synthesized by EDC/NHS binding of heparin with carboxylated poloxamer. The chemical structure of the synthesized HEP copolymers was evaluated comparatively with the poloxamer (POL) and untreated heparin with respect to FTIR spectra. The characteristic peak of POL observed at 2887 cm^{-1} is consistent with the reported range of 2785–3005 cm^{-1}.[11] The FTIR spectra of HEP1, HEP2, and HEP3 exhibited the characteristic POL peak at 2887, 2878, and 2888 cm^{-1}, respectively. Additionally, new characteristic bands in the 1115–1735 cm^{-1} range, which belong to the carbonyl vibration of HEP[22] was observed, verifying the successful conjugation of heparin. Moreover, the broad absorption peaks assigned to the stretching vibration of hydroxyl groups from heparin residues appeared at around 3473 and 3458 cm^{-1}, which are in agreement with the absorption peak of untreated heparin at 3413 cm^{-1}.[30] According to the toluidine blue assay ($ABS_{@629}$), conjugated heparin amounts per gram of HEP1, HEP2, and HEP3 were 1.986, 2.010, and 2.022 mg, respectively (Figure 1a). The equation of the calibration curve was calculated as $y = -0,0431x + 0,1377$ ($R^2 = 0.9953$), where the absorbance was y and the concentration of heparin was x. Increasing the mass ratio of heparin to carboxylated poloxamer in the conjugation reaction medium could not significantly increase the conjugation efficiency, probably because heparin, which can be bound to active carboxyl groups of carboxylated poloxamer, was selected at a feed concentration close to reaction saturation. Hence, only one of them (HEP3) (bearing the highest heparin) was used for all rheological and cytotoxic investigations.

Thus, rheological characterizations and bioactivity assays were only carried out with HEP3. Three-dimensional (3D) porosity images and pore volumes of POL and HEP3 hydrogels at a concentration of 25% (w/v) were obtained by micro-computed tomography (µ-CT) analyses (Figure 1b-a). The majority of pore sizes of POL and HEP3 were not statistically different ($p < 0.05$) and found as 65.17 ± 1.41% and 65.16 ± 3.28%, respectively at 0.0200 mm. Pores of other size ranges and their percentages were also similar for POL and HEP3 ($p < 0.05$). (Figure 1b-b). The mean pore sizes
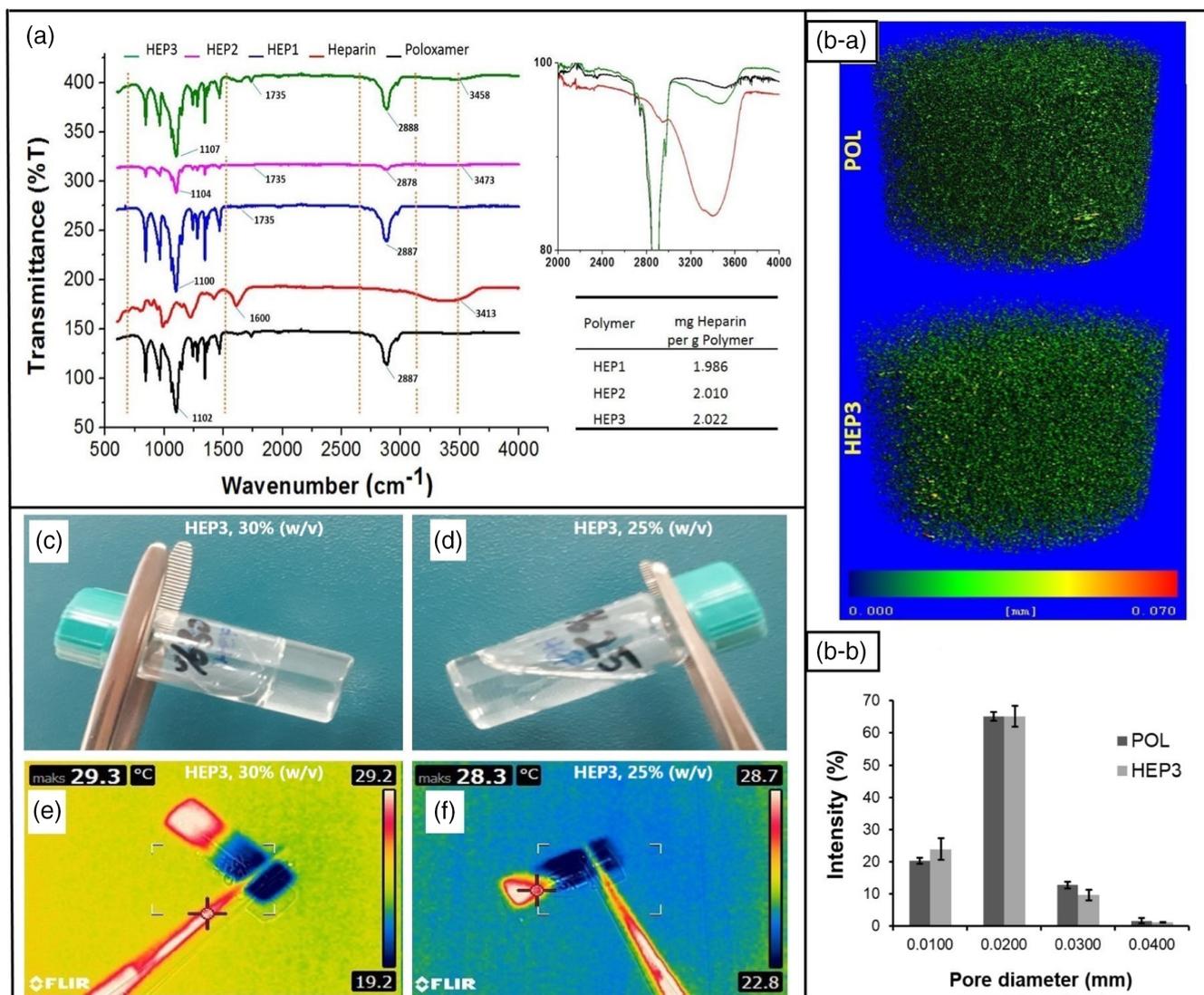
FIGURE 1   FTIR spectra of poloxamer, untreated heparin, HEP1, HEP2, and HEP3 along with the related conjugated-heparin amounts per g of poloxamer based on toluidine blue test (a). 3D images of micro-computed tomography analyses of POL and HEP3 at the concentration of 25% (w/v) (b). At room temperature, HEP3 at the concentration of 30% exhibits gel form (c), whereas it exhibits fluid form at the concentration of 25% (d). Thermal images of HEP3 at the concentration of 30% (e) and 25% (f). [Color figure can be viewed at wileyonlinelibrary.com]

were 0.0196 ± 0.0064 mm and 0.0188 ± 0.0061 mm for POL and HEP3, respectively ($p < 0.05$). These porosity results are consistent with another study, where the porosity of 25% (w/w) P407 hydrogel was measured as 60% at 0.02 mm, which was reported to be suitable for cell proliferation.[26] In another study, μ-CT analysis of SAG-based hydrogel produced for bone damage showed that the porosity and pore size of the hydrogel resembled a natural ECM required for implants with pore sizes of about 200–550 μm, found to be favorable for cell mobility and nutrient transport.[31] The thermo-responsive hydrogels showed fluid-like behavior below their specific gelation temperatures, while exhibiting gel-like behavior at temperatures above. Real and thermal camera images of HEP3 at the concentration

of HEP3 30% (w/v) showed its gel-like non-fluidal appearance at room temperature (Figure 1c,e), whereas HEP3 at the concentration of 25% (w/v) has liquid-like property (Figure 1), indicating ease of injectability.

3.2 | Determination of rheological properties

Evaluation of the viscosity as a function of temperature allows monitoring of the gelation temperature of hydrogels, and the sol–gel transition occurs as soon as the elastic gel-like behavior appears.[11] In this study, the gelation temperatures of POL and HEP3 hydrogels were

	Concentration (w/v)	Gelation temperatures (°C)	
		Viscometer	Magnetic stirrer method
POL	20%	28.0	28.2
	25%	23.1	23.1
	30%	20.7	20.4
HEP3	20%	42.0	42.0
	25%	29.8	30.0
	30%	22.2	22.0

TABLE 1 Gelation temperatures of POL and HEP3 hydrogels at three different concentrations according to the magnetic stirrer and viscosimeter.

investigated at three different concentrations of 20%, 25%, and 30% (w/v) by using both magnetic stirrer and viscosimeter. The results obtained with these two measurement methods were quite similar, confirming each other (Table 1).

According to the viscosity analyses, gelation temperatures of POL at concentrations of 20%, 25%, and 30% (w/v) were determined as 28.0, 23.1, and 20.7°C, respectively. In addition, the gelation temperatures were validated by the magnetic stirrer method, where the transition of POL at concentrations of 20%, 25%, and 30% (w/v) from liquid-like behavior to elastic gel-like behaviors occurred at 28.2, 23.1, and 20.4°C, yielding similar results. As such, the gelation temperatures of HEP3 at concentrations of 20%, 25%, and 30% (w/v) were determined as 42.0, 29.8, and 22.2°C by the viscometer (Figure 2a,b), whereas 42.0, 30.0, and 22.0°C by the magnetic stirrer method, respectively. As the thermoresponsive gelation is due to hydrophobic interactions between the copolymer chains of poloxamer, decreasing the concentration probably caused weaker hydrophobic interactions resulting in gelation at higher temperatures.[32] Moreover, heparin conjugation may hinder hydrophobic interactions between copolymer chains as sulfate groups in heparin are potential participants of the intermolecular hydrogen bonding between heparin and copolymer chains.[33] So, gelation temperatures of HEP3 were higher than the POL at the same concentrations consistent with previous studies with respect to heparin-modified hydrogels.[22,25]

Rheological properties were evaluated by Rheometer (Discovery HR-2, Hybrid rheometer) characterizing the viscoelastic nature of 25% (w/v) POL and HEP3 hydrogels. The storage and loss moduli were examined as functions of strain (0.01–1000%) and frequency (0.01–100 Hz) for the self-healing behavior of the hydrogels and the confirmation of the hydrogel behavior, respectively. The oscillation amplitude test was performed to ascertain the region where the hydrogels undergo deformation. The oscillation amplitude sweep tests of POL and HEP3 hydrogels showed similar critical strains of about 5.6%

(Figure 2c). Although the difference between storage and loss moduli was noticeable, it did not affect the critical strain value. When the strain was increased up to 5.6%, the values of storage modulus started to decrease while loss modulus started to increase for both hydrogels. At the oscillation strain of 5.6%, the values of storage modulus were 370.74 and 236.74 Pa for POL and HEP3, respectively, while values of loss modulus were 16.0 and 17.6 Pa for POL and HEP3, respectively. Hence, it can be understood from the oscillation-strain tests that the storage modulus of poloxamer hydrogel decreased with the ratio of 36.14% after heparin conjugation. Based on the results, the softness of the hydrogels is convenient for biological applications.[34] According to the oscillation frequency test, the complex viscosities of POL and HEP3 were 58.63 and 31 Pa.s, at a shear strain of 1% and a frequency of 1 Hz. In the other words, the complex viscosity of POL was higher than that of HEP3. The values of the storage and loss modulus were 364 and 12.46 Pa for POL, and 196 and 16.57 Pa for HEP3, respectively. When the storage and loss modulus were studied as frequency-dependent, storage modulus was dominant over the entire frequency range (0.01–100 Hz, Figure 2d), supporting the hydrogel-like behavior.[35] Additionally, as in the oscillation amplitude test, the storage modulus value was higher, whereas the loss modulus value was lower in POL compared to HEP3 in the oscillation frequency test. As POL has a higher difference between loss and storage modules, the friction of the temporomandibular joint could be high and require more energy if utilized as a biomaterial to support load-bearing jaw movement. Hence, HEP3 has been considered superior to pristine poloxamer causing more fatigue in the muscles as an injectable hydrogel for the temporomandibular cavity.

Step-strain measurements (TOST) were performed in the range of the high strain (400%) for 100 s to disrupt the hydrogel structure and the lower strain (1%) for the next 100 s as the behavior of the hydrogel subjected to high strain is critical for injectability.[36] Strain-recovery between alternating high and low strain cycles of both hydrogels revealed full recovery of the gel network
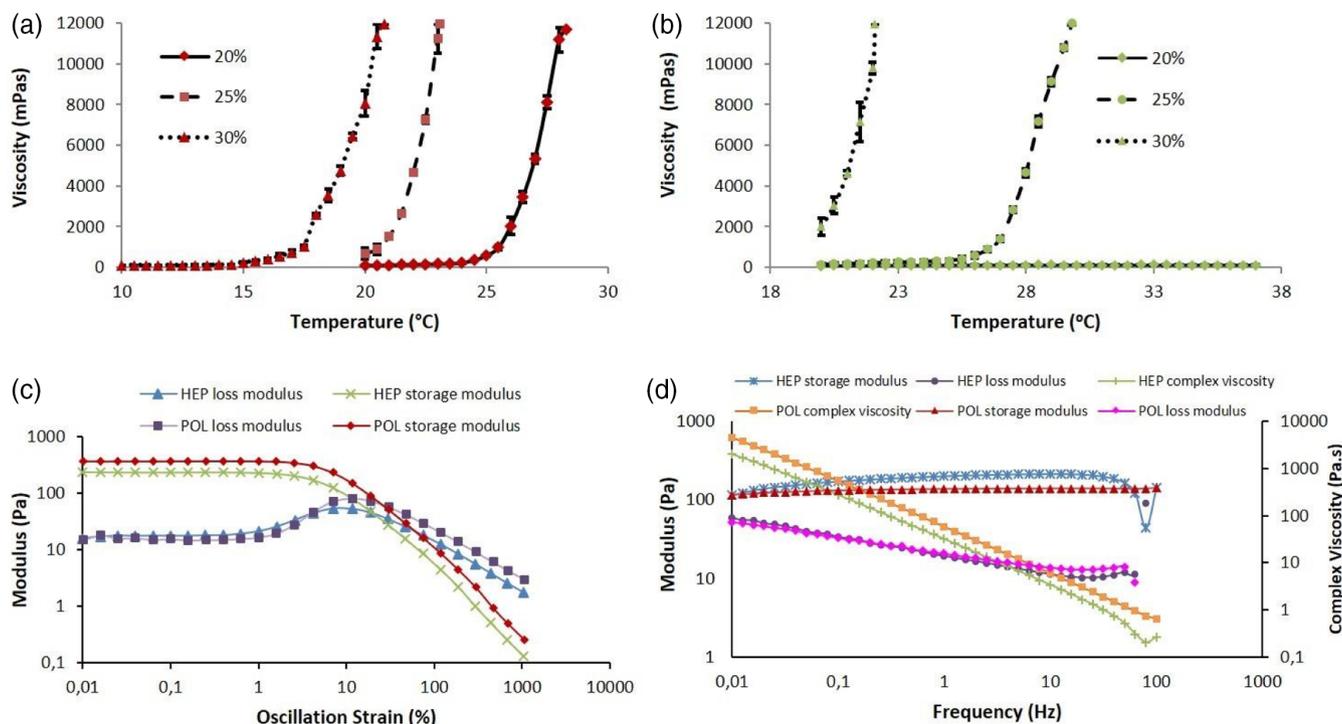
FIGURE 2 Temperature-dependent viscosity measurement results of POL (a) and HEP3 (b) hydrogels at concentrations of 20%, 25%, and 30%. Oscillation strain dependent storage and loss modulus for POL and HEP3 according to oscillation amplitude test (c). Frequency dependent modulus and complex viscosity plot for POL and HEP3 (d). [Color figure can be viewed at wileyonlinelibrary.com]

without notable reduction of the average magnitude of storage and loss moduli, displaying a remarkable and rapid thixotropic behavior. POL and HEP3 hydrogels have returned to their former states quite quickly and without losing their properties in second cycles (Figure 3a,b), indicating that the structures of the gels are robust and reversible.

Creep and recovery tests were performed by applying different shear stresses to determine time-dependent viscoelastic deformation, where the first 400 s represents load application as creep test and later 1200 s, load removal as recovery test. Initial deformation determines the end of the elastic stage and the beginning of the viscoelastic stage, and the plateau represents the viscous stage. When the load is removed, there is an elastic recovery with chain molecule rearrangement, resulting in a final permanent deformation.[37] The proximity of max interaction zones in POL was due to the lower storage module value. The total creep strain after loading was approximately 5% for POL (Figure 3c) and 8% for HEP3 (Figure 3d), the low strain value for POL was due to its higher storage modulus compared to HEP3. Moreover, the recoverable strain (composed of elastic strain and viscoelastic strain components) or in the other words, the elastic recovery percentage (R) value of POL was lower than the recoverable strain of HEP3 (Figure 3e). The shear creep compliance (J), which can be divided into

three parts as instantaneous elastic (J_o), the delayed elastic (J_d) and viscous (J_∞) components, relates to sample softness. The larger maximum deformation in creep interval (J_{max}) value represents the weaker material structure. These values were compatible with the relationship of loss modules in oscillation frequency testing. Thus, it can be concluded that POL has a higher elastic structure with a lower J value. However, the total elastic recovery percentage was higher for HEP3, indicating that the gel shows higher elastic recoverability by better correction of the deformed structure.

The elastic recoverability tests of hydrogels are very important for investigating the mechanical viscoelastic behavior of biomaterials. All applications of biomaterials require optimum recoverability properties and maximum performance under load. Figure 4 gives some information about POL and HEP3 hydrogels and explains the deformation properties of hydrogels under constant stress time. According to the time scanning test under a certain load, both POL and HEP3 hydrogels returned to their former structures with only little deformation over time. However, it should be noted that less time was needed for HEP3 to return its former state (Figure 4a). When stress was applied to the hydrogels, both showed similar characteristic deformation slopes. However, different moduli values were obtained. These differences could be explained by the oscillation strain test, which showed
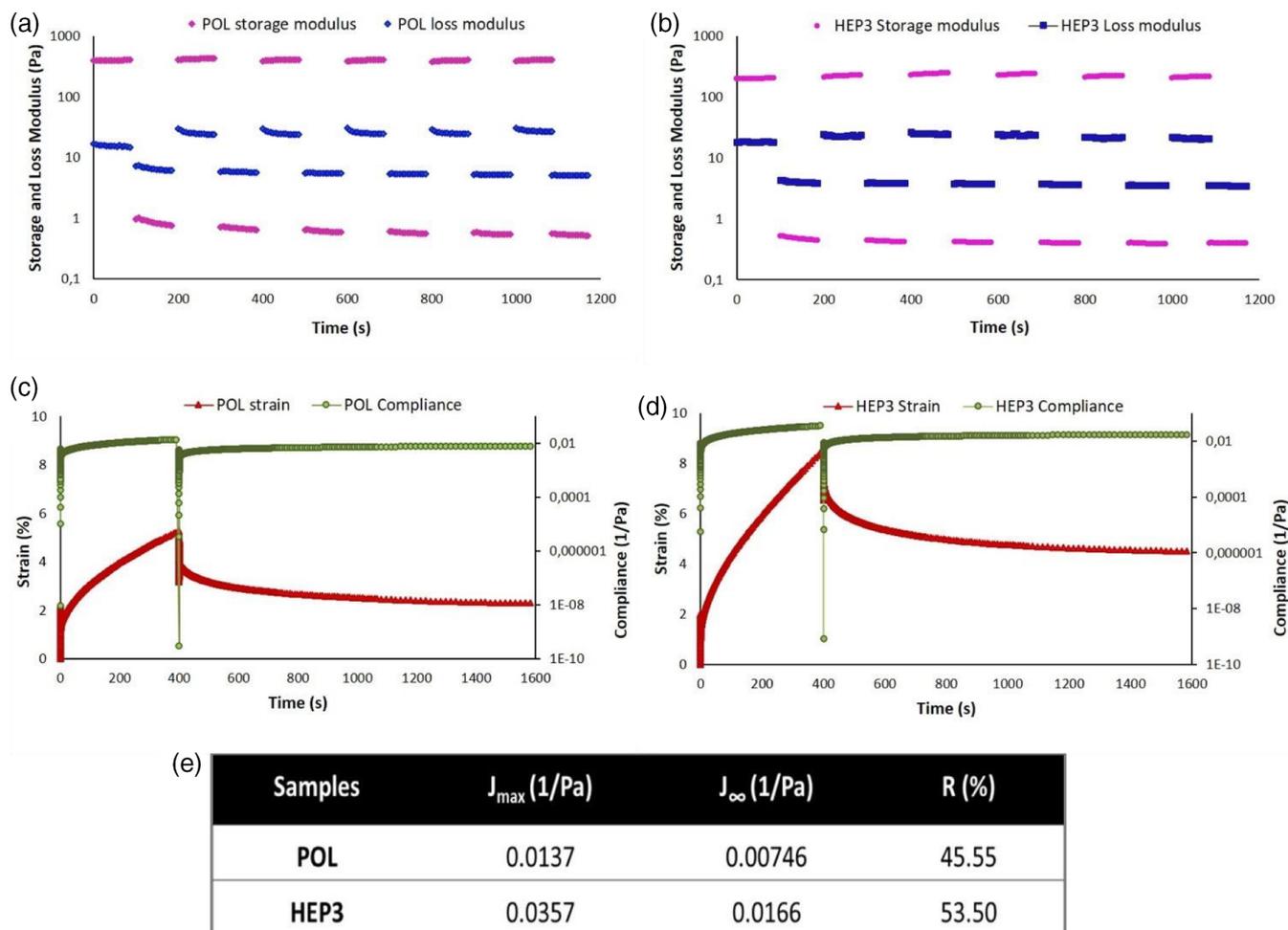
FIGURE 3 Time dependent storage and loss modules values obtained from step-strain test for POL (a) and HEP3 (b). Time dependent shear strain and compliance plot for POL (c) and HEP3 (d). Max deformation in creep interval (J_{max}), viscous complement (J_∞) and elastic recovery percentage (R) values derived from the flow test (e). [Color figure can be viewed at wileyonlinelibrary.com]

storage modulus differences in the linear viscoelastic region of the graph. The storage modulus of HEP3 hydrogel was lower than that of POL. The deformation of hydrogel properties under shear rates changed between 0.1 and 1000 1/s (Figure 4b), and the correlation factors (R^2) of the flow curves were calculated as 0.816585 and 0.792050, while fluidity index values were 0.368877 and 0.0273684 for the POL and HEP3, respectively. These values indicate that gels are compatible with the Herschel-Bulkley model, which refers to the nonlinear relationship of the tension of a non-Newtonian fluid with stress. In non-Newtonian fluids, the shear rate ratio changes between the shear stresses that make up the viscosity as 0 or nonlinear. In the Herschel-Bulkley model, the fluidity index (n) is known to extend from 0 to 1.[38]

The flow thixotropic behaviors of hydrogels yield information about the recoverability of hydrogels. That is, how hydrogels return to their original shapes and how much deformation occurs after injection into temporomandibular

joint with a very high shear rate. Thixotropy tests revealed the time-dependent shear thinning properties of POL and HEP3 hydrogels showing the reversible structural transition. The loop size increased with decreasing elastic recovery under variable shear rates, indicating the effects of the injection process on the mechanical properties of hydrogels. HEP3 hydrogel has a higher cycle loop area than the POL hydrogel (Figure 4c) and a greater reduction at the second range of shear rates. As the loop area is a sign of the extent of thixotropic nature, which also shows the energy consumed in the structural breakdown of a material, it is thought that HEP3 has a better ability to reform the damaged structure by van der Walls forces of attraction.[39] The binary polymer blends of Poloxamer 407 and Carbopol 971P® were reported to exhibit significantly increased thixotropy area which attributed to indicative of a higher time for the structure return to the relaxed molecular configuration, greater flexibility, fracture resistance, compared to the poloxamer alone.[40]
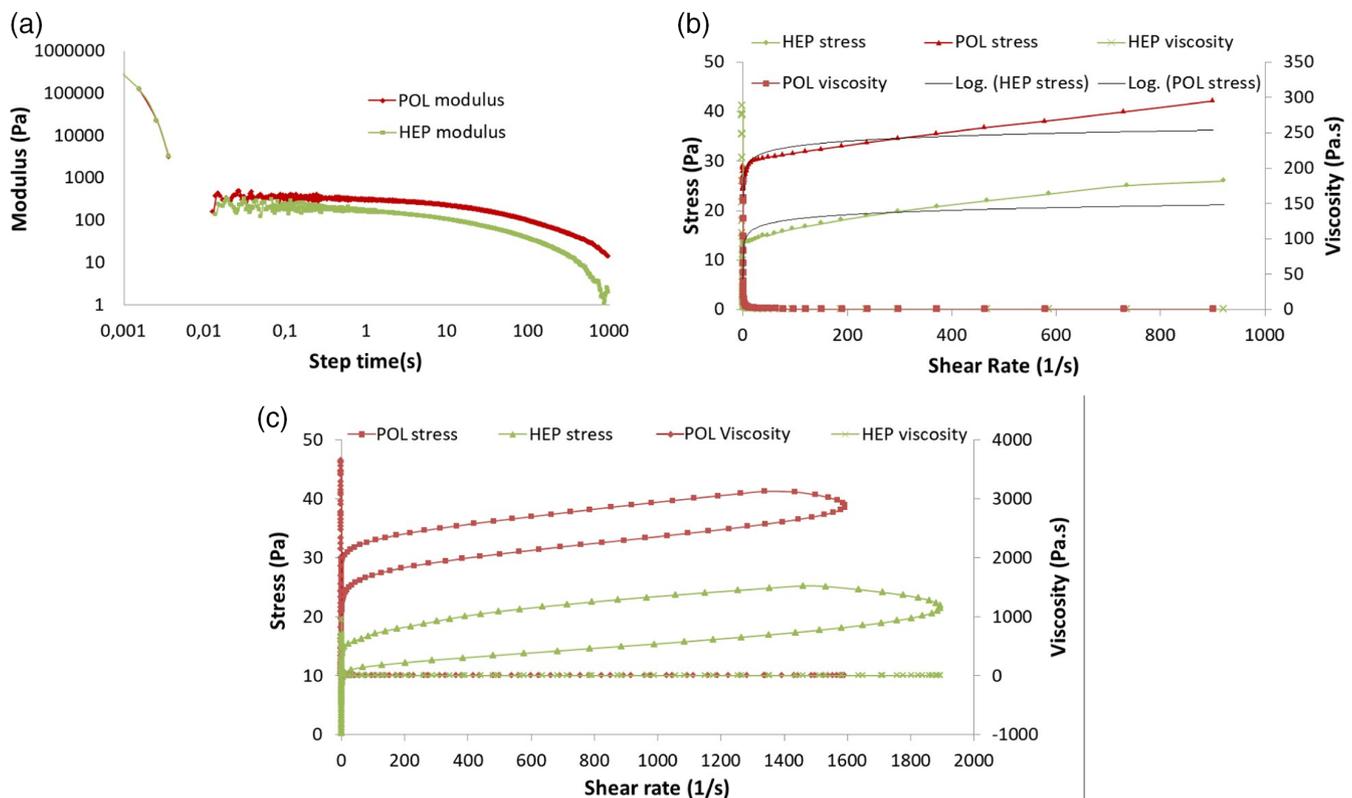
FIGURE 4 Time dependent module graph (a), and shear rate-stress-viscosity plots both of POL and HEP3 obtained by flow test 1 (b) and flow test 2 (c). [Color figure can be viewed at wileyonlinelibrary.com]

3.3 | Biocompatibility of hydrogels

The results of MTT test that was performed to determine the cytotoxic effect of different concentrations of POL and HEP3 hydrogels on L929 and ATDC5 cells, was shown in Figure 5a,b. While the cell viabilities of all concentrations of POL and HEP3 were above 70% (safety range) for both L929 and ATDC5 cells at the end of 72 h, all concentrations of two hydrogels increased L929 cell proliferation (cell viability was above 100%) compared to control group, with a significantly ($p < 0.0001$) high concentration of (0.0313 mg/ml) POL, mainly. Besides, it was observed that ATDC5 cell proliferation was increased significantly with HEP3 in increasing concentrations up to 0.0156 mg/ml ($p < 0.0001$) compared to POL and the control group. As can be seen in most applications, further increase in HEP3 concentration led to a critical decrease in cell proliferation. When the concentration of biocompatible materials increases, generally cell proliferation increases as well. However, sometimes there may not be a significant correlation, or after a certain point, high concentrations can reverse the proliferation by causing a toxic effect, depending on the interactions in the mixture produced and the mechanism of action of the components. This is why ideal dose determination is so important. Thus, the highest cell viabilities for both L929 and ATDC5 cells was determined at concentrations of 0.0313 mg/ml for POL ($p < 0.0001$; $p < 0.05$, respectively) and 0.0156 mg/ml for HEP3 ($p < 0.0001$; $p < 0.0001$, respectively). It could be understood from the results, hydrogel functionalization with heparin supports chondrocyte cell viability and proliferation for tissue regeneration. Previous studies have shown that heparin can stimulate osteogenesis[41,42] and promote proliferation and osteogenic differentiation by Wnt signaling.[43] However, limited studies have been reported on the use of heparin-containing hydrogels for chondrogenesis in cartilage tissue engineering.[44] In one of them, it has been shown that the presence of heparin in hydrogels promotes chondrocyte proliferation and differentiation for cartilage regeneration,[45] while another has been reported the appropriate environment for cartilage tissue formation from chondrocytes could be provided by heparin based hydrogel.[46] The Live&Dead analysis results were consistent with MTT results (Figure 5c-f and Figure S2). It has been clearly seen that live cells were more than dead cells for both cell types. Additionally, the dead cell densities of HEP3 hydrogel groups were less than POL counterparts. Due to the physicochemical and biocompatible properties, poloxamer/heparin-based hydrogels are used in tissue engineering and biomedical studies.

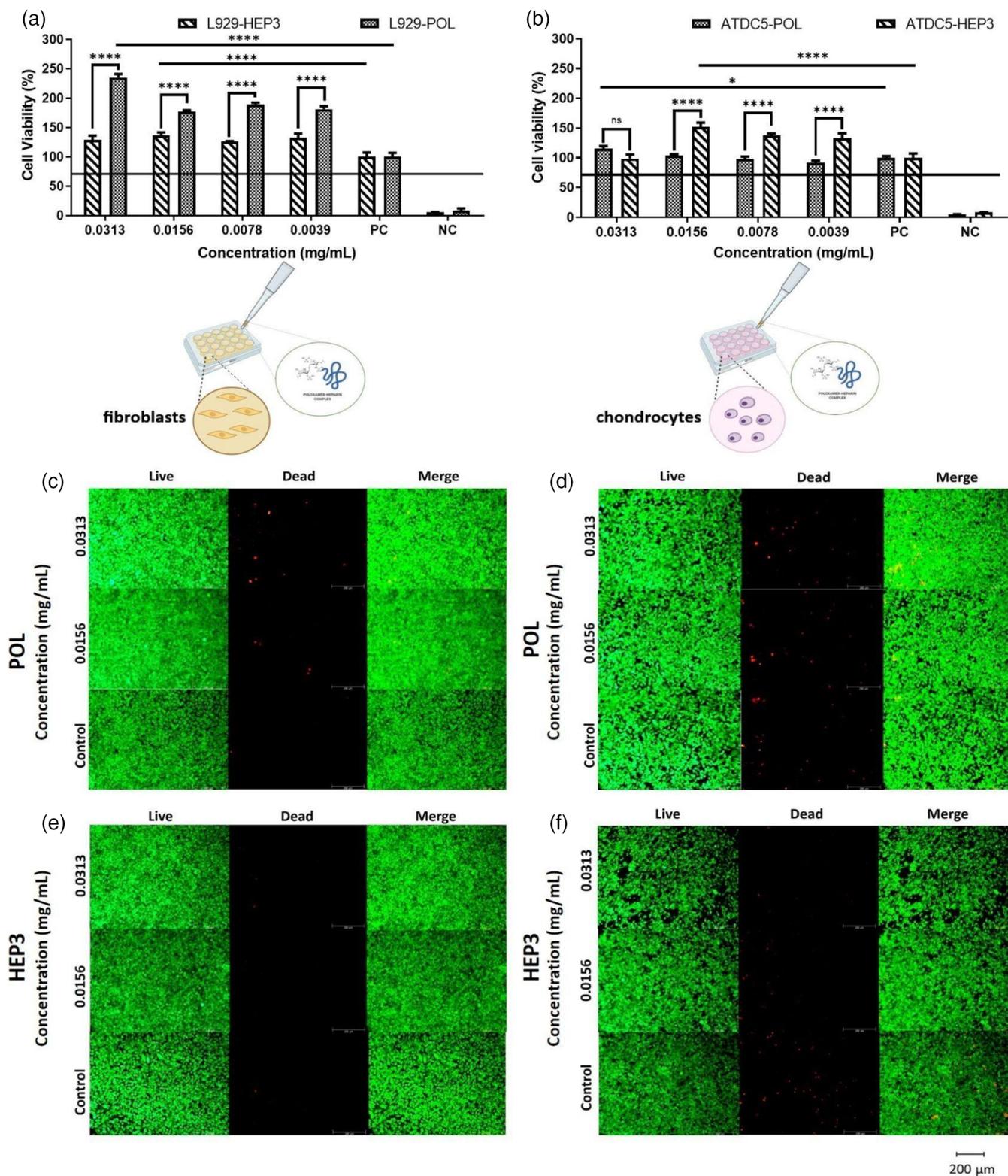Double networked poloxamer-heparin/gellan gum hydrogels have been shown to allow cell proliferation

FIGURE 5 Percent cell viabilities of POL and HEP3 for L929 (a) and ATDC5 cell lines (b) at different concentrations (ns;p > 0.05, *p < 0.05, ****p < 0.001). Based on Live&Dead staining test, the cell viability images of L929 (c) and ATDC5 (d) cell lines treated with POL at different concentrations had shown together with the cell viability images of L929 (e) and ATDC5 (f) cells treated with HEP3 at different concentrations. "PC" denotes only nutrient medium as positive control and "NC" denotes DMSO as negative control. (L929, ATDC5 cell and well-plate images were created in BioRender.com). [Color figure can be viewed at wileyonlinelibrary.com]

and osteogenic differentiation of BMSCs when used in cell delivery studies.[11] In another study, a hydrogel encapsulated with heparin and bFGF was shown to accelerate in vitro HIN3T3 cell survival and the healing of chronic wounds in rats, due to vascularization and reduced inflammation effect of heparin.[16] Additionally, basic fibroblast and nerve growth factors added to heparin-poloxamer hydrogels were reported to provide effective therapeutic strategies for spinal cord injury repair, via improving neuronal survival, axon regeneration, reactive astrogliosis suppression and locomotor recovery.[47] Moreover, growth inhibition efficacy of doxorubicin loaded heparinized poloxamer hydrogels and doxorubicin loaded pristine P407 polymer were studied as a drug entrapmenter against murine sarcoma cancer cell line (S180), where the results showed that the anticancer effect of heparin containing groups were higher than the corresponding groups in the absence of heparin.[22]

4 | CONCLUSIONS

The present work demonstrates the injectable design of heparin conjugated poloxamer hydrogel with temperature sensitive in situ gelation at the TMJ disc disorders. This study according to our knowledge is the first in which suitability of polymeric hydrogel functionalized with heparin, a member of the glycosaminoglycan family of sulfated polysaccharides, as an injectable displacement biomaterial for TMJ disc has been examined in terms of viscoelastic properties and cytotoxicity. The results showed that the contribution of heparin improved the biomechanical properties while both hydrogels with/without heparin were not already cytotoxic at the desired concentrations for the TMJ cavity. In conclusion, HEP3 hydrogel is predicted to be a promising biomaterial and can further be tested in vivo for the treatment of TMJ disorders.

AUTHOR CONTRIBUTIONS
Buse Deliogullari: Data curation (lead); formal analysis (lead); validation (equal); writing – original draft (equal). **Esra Ilhan-Ayisigi:** Conceptualization (supporting); data curation (supporting); formal analysis (supporting); methodology (supporting); writing – original draft (equal). **Betul Cakmak:** Data curation (supporting); methodology (supporting); validation (supporting); visualization (supporting); writing – original draft (supporting). **Pelin Saglam-Metiner:** Data curation (supporting); formal analysis (equal); software (equal); visualization (equal); writing – original draft (supporting). **Nusret Kaya:** Data curation (equal); formal analysis (supporting); methodology (supporting); supervision (supporting); validation (supporting). **Gulcan Coskun-Akar:** Formal analysis (supporting); methodology (supporting); supervision (supporting); validation (supporting); writing – review and editing (supporting). **Ozlem Yesil-Celiktas:** Conceptualization (lead); funding acquisition (lead); methodology (supporting); supervision (lead); writing – review & editing (lead).

DATA AVAILABILITY STATEMENT
The data that support the findings of this study are available in the supplementary material of this article.

ORCID
Buse Deliogullari https://orcid.org/0000-0003-0539-7548
Esra Ilhan-Ayisigi https://orcid.org/0000-0003-1880-4261
Betul Cakmak https://orcid.org/0000-0003-1247-6295
Pelin Saglam-Metiner https://orcid.org/0000-0002-5726-1928
Nusret Kaya https://orcid.org/0000-0003-1727-3155
Gulcan Coskun-Akar https://orcid.org/0000-0002-9343-9228
Ozlem Yesil-Celiktas https://orcid.org/0000-0003-4509-2212

REFERENCES
[1] S. Fazaeli, S. Ghazanfari, V. Everts, T. H. Smit, J. H. Koolstra, *Osteoarthr. Cartil.* **2016**, *24*, 1292.
[2] N. Jiang, Y. Yang, L. Zhang, Y. Jiang, M. Wang, S. Zhu, *J. Dent. Res.* **2021**, *100*, 839.
[3] E. Tanaka, T. van Eijden, *Crit. Rev. Oral Biol. Med.* **2003**, *14*, 138.
[4] T. M. Acri, K. Shin, D. Seol, N. Z. Laird, I. Song, S. M. Geary, J. L. Chakka, J. A. Martin, A. K. Salem, *Adv. Healthcare Mater.* **2019**, *8*, 1.
[5] K. Dashnyam, J. H. Lee, N. Mandakhbayar, G. Z. Jin, H. H. Lee, H. W. J. Kim, *Tissue Eng.* **2018**, *9*, 2041731418776514.
[6] E. Tanaka, M. S. Detamore, L. G. Mercuri, *J. Dent. Res.* **2008**, *87*, 296.
[7] F. Liu, A. Steinkeler, *Dent. Clin. North Am.* **2013**, *57*, 465.

[8] A. H. H. Talasaz, A. A. Ghahremankhani, S. H. Moghadam, M. R. Malekshahi, F. Atyabi, R. Dinarvand, *J. Appl. Polym. Sci.* **2008**, *109*, 2369.

[9] X. Zhao, D. K. Debeli, G. Shan, *J. Appl. Polym. Sci.* **2020**, *137*, 48669.

[10] K. Phogat, S. Kanwar, D. Nayak, N. Mathur, S. B. Ghosh, S. Bandyopadhyay-Ghosh, *J. Appl. Polym. Sci.* **2020**, *137*, 48789.

[11] J. H. Choi, O. K. Choi, J. Lee, J. Noh, S. Lee, A. Park, M. A. Rim, R. L. Reis, G. Khang, *Colloids Surf. B Biointerf.* **2019**, *181*, 879.

[12] G. Dumortier, J. L. Grossiord, F. Agnely, J. C. Chaumeil, *Pharm. Res.* **2006**, *23*, 2709.

[13] J. H. Park, J. K. Yoon, Y. J. Kim, T. J. Lee, G. J. Jeong, D. I. Kim, S. H. Bhang, *J. Ind. Eng. Chem.* **2019**, *80*, 846.

[14] H. Kweon, M.-K. Yoo, J.-H. Lee, W.-R. Wee, Y.-G. Han, K.-G. Lee, C.-S. Cho, *J. Appl. Polym. Sci.* **2003**, *88*, 2670.

[15] H. H. Jung, K. Park, D. K. Han, *J. Controlled Release* **2010**, *147*, 84.

[16] J. Peng, H. Zhao, C. Tu, Z. Xu, L. Ye, L. Zhao, Z. Gu, D. Zhao, J. Zhang, Z. Feng, *Mater. Sci. Eng. C* **2020**, *116*, 111169.

[17] Y. Z. Zhao, H. F. Lv, C. T. Lu, L. J. Chen, M. Lin, M. Zhang, X. Jiang, X. T. Shen, R. R. Jin, J. Cai, X. Q. Tian, H. L. Wong, *PLoS One* **2013**, *8*, 1.

[18] M. Kim, Y. H. Kim, G. Tae, *Acta Biomater.* **2013**, *9*, 7833.

[19] Y. Luo, L. Fan, C. Liu, H. Wen, S. Wang, P. Guan, D. Chen, C. Ning, L. Zhou, G. Tan, *Bioact. Mater.* **2022**, *7*, 98.

[20] E. Saygili, E. Kaya, E. Ilhan-Ayisigi, P. Saglam-Metiner, E. Alarcin, A. Kazan, E. Girgic, Y.-W. Kim, K. Gunes, G. G. Eren-Ozcan, D. Akakin, J.-Y. Sun, O. Yesil-Celiktas, *Int. J. Biol. Macromol.* **2021**, *172*, 381.

[21] Z. Wu, S. Korntner, A. Mullen, D. Zeugolis, *Biomater. Biosyst.* **2021**, *4*, 100030.

[22] J. Li, H. Pan, S. Qiao, Y. Li, J. Wang, W. Liu, W. Pan, *Int. J. Biol. Macromol.* **2019**, *134*, 63.

[23] K. T. Nguyen, T. H. Nguyen, D. H. Do, Q. H. Le, *Adv. Nat. Sci. Nanosci. Nanotechnol.* **2017**, *8*, 015002.

[24] S. Bobbala, B. Gibson, A. B. Gamble, A. McDowell, S. Hook, *Immunol. Cell Biol.* **2018**, *96*, 656.

[25] J. L. Tian, Y. Z. Zhao, Z. Jin, C. T. Lu, Q. Q. Tang, Q. Xiang, C. Z. Sun, L. Zhang, Y. Y. Xu, H. S. Gao, Z. C. Zhou, X. K. Li, Y. Zhang, *Drug Dev. Ind. Pharm.* **2010**, *36*, 832.

[26] Y. Gezgin, A. Kazan, F. Ulucan, O. Yesil-Celiktas, *Ind. Crops Prod.* **2019**, *139*, 111588.

[27] M. Fidan-Yardimci, S. Akay, F. Sharifi, C. Sevimli-Gur, G. Ongen, O. Yesil-Celiktas, *Food Chem.* **2019**, *293*, 57.

[28] M. E. Blewis, G. E. Nugent-Derfus, T. A. Schmidt, B. L. Schumacher, R. L. Sah, *Eur. Cells Mater.* **2007**, *13*, 26.

[29] E. Ilhan-Ayisigi, F. Ulucan, E. Saygili, P. Saglam-Metiner, S. Gulce-Iz, O. Yesil-Celiktas, *J. Sci. Food Agric.* **2020**, *100*, 3525.

[30] Z. Zhi, J. Li, J. Chen, S. Li, H. Cheng, D. Liu, X. Ye, R. J. Linhardt, S. Chen, *Ultrason. Sonochem.* **2019**, *52*, 184.

[31] L. Xu, X. Bai, J. Yang, J. Li, J. Xing, H. Yuan, J. Xie, J. Li, *Int. J. Biol. Macromol.* **2020**, *165*, 2964.

[32] A. Fakhari, M. Corcoran, A. Schwarz, *Heliyon* **2017**, *3*, e00390.

[33] Y.-I. Chung, S.-Y. Lee, G. Tae, *Colloids Surfaces A Physicochem. Eng. Asp.* **2006**, *284–285*, 480.

[34] Q. Wang, Y. He, Y. Zhao, H. Xie, Q. Lin, Z. He, X. Wang, J. Li, H. Zhang, C. Wang, F. Gong, X. Li, H. Xu, Q. Ye, J. Xiao, *ACS Appl. Mater. Interfaces* **2017**, *9*, 6725.

[35] E. A. Appel, M. W. Tibbitt, M. J. Webber, B. A. Mattix, O. Veiseh, R. Langer, *Nat. Commun.* **2015**, *6*, 6295.

[36] S. Morariu, M. Bercea, L. Sacarescu, *Ind. Eng. Chem. Res.* **2014**, *53*, 13690.

[37] F. M. Monticeli, H. L. Ornaghi, R. M. Neves, M. Odila Hilário Cioffi, *J. Strain Anal. Eng. Des.* **2020**, *55*, 109.

[38] G. Mullineux, *Appl. Math. Model.* **2008**, *32*, 2538.

[39] I. Ali, L. A. Shah, *Polym. Bull.* **2021**, *78*, 1275.

[40] S. B. De Souza Ferreira, T. D. Moço, F. B. Borghi-Pangoni, M. V. Junqueira, M. L. Bruschi, *J. Mech. Behav. Biomed. Mater.* **2015**, *55*, 164.

[41] D. Li, Z. Yang, X. Zhao, Y. Luo, W. Zhou, J. Xu, Z. Hou, P. Kang, M. Tian, *Chem. Eng. J.* **2022**, *435*, 134991.

[42] M. Simann, V. Schneider, S. Le Blanc, J. Dotterweich, V. Zehe, M. Krug, F. Jakob, T. Schilling, N. Schütze, *Bone* **2015**, *78*, 102.

[43] L. Ling, E. T. Camilleri, T. Helledie, R. M. Samsonraj, D. M. Titmarsh, R. J. Chua, O. Dreesen, C. Dombrowski, D. A. Rider, M. Galindo, I. Lee, W. Hong, J. H. Hui, V. Nurcombe, A. J. van Wijnen, S. M. Cool, *Gene* **2016**, *576*, 292.

[44] J. Chen, A. Chin, A. J. Almarza, J. M. Taboas, *Biomed. Mater.* **2020**, *15*, 045006.

[45] R. Jin, L. S. Moreira Teixeira, P. J. Dijkstra, C. A. van Blitterswijk, M. Karperien, J. Feijen, *J. Controlled Release* **2011**, *152*, 186.

[46] M. Kim, Y. Shin, B.-H. Hong, Y.-J. Kim, J.-S. Chun, G. Tae, Y. H. Kim, *Methods* **2010**, *16*, 1.

[47] X. Hu, R. Li, Y. Wu, Y. Li, X. Zhong, G. Zhang, Y. Kang, S. Liu, L. Xie, J. Ye, J. Xiao, *J. Cell. Mol. Med.* **2020**, *24*, 8166.

SUPPORTING INFORMATION

Additional supporting information may be found in the online version of the article at the publisher's website.